

RSC Advances



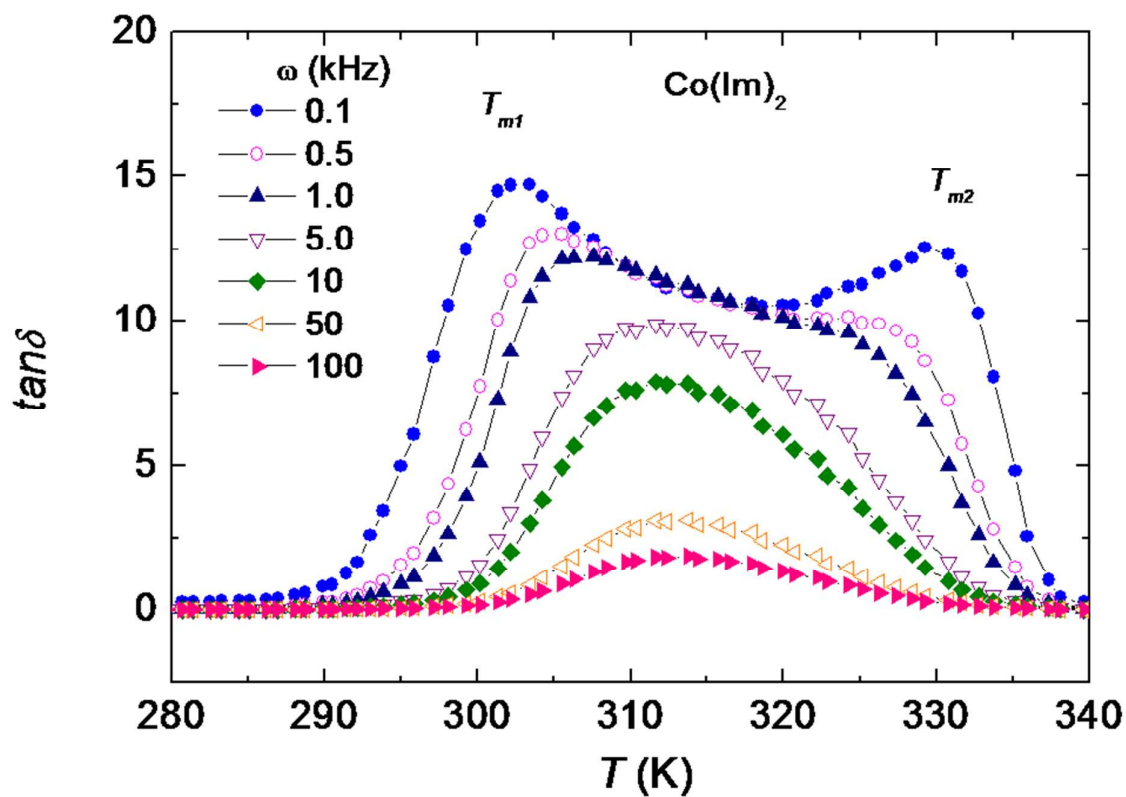
This is an *Accepted Manuscript*, which has been through the Royal Society of Chemistry peer review process and has been accepted for publication.

Accepted Manuscripts are published online shortly after acceptance, before technical editing, formatting and proof reading. Using this free service, authors can make their results available to the community, in citable form, before we publish the edited article. This *Accepted Manuscript* will be replaced by the edited, formatted and paginated article as soon as this is available.

You can find more information about *Accepted Manuscripts* in the [Information for Authors](#).

Please note that technical editing may introduce minor changes to the text and/or graphics, which may alter content. The journal's standard [Terms & Conditions](#) and the [Ethical guidelines](#) still apply. In no event shall the Royal Society of Chemistry be held responsible for any errors or omissions in this *Accepted Manuscript* or any consequences arising from the use of any information it contains.

Graphical Abstract



Dielectric relaxation phenomenon with non-Debye dynamics in $\text{Co(CO}_3\text{)(H}_2\text{O)}_2\text{(C}_3\text{H}_4\text{N}_2\text{)}_2$ and $[\text{Co(C}_3\text{H}_3\text{N}_2\text{)}_2]_n$, resemble to the behaviour of ferroelectric relaxors is presumably connected with the charge carriers.

DOI: ((will be filled in by the editorial staff))

Dielectric properties of $\text{Co}(\text{CO}_3)(\text{H}_2\text{O})_2(\text{C}_3\text{H}_4\text{N}_2)_2$ and $[\text{Co}(\text{C}_3\text{H}_3\text{N}_2)_2]_n$

B. Świątek-Tran^[a], H. A. Kołodziej^[b], A. Vogt^[b] and V. H. Tran^[c]

((Dedication, optional))

We have investigated the dielectric permittivity (ϵ' , ϵ'') of $\text{Co}(\text{CO}_3)(\text{H}_2\text{O})_2(\text{C}_3\text{H}_4\text{N}_2)_2$ and two samples of $[\text{Co}(\text{C}_3\text{H}_3\text{N}_2)_2]_n$ at low frequencies (0.1 – 1000 kHz) and in the temperature range 80 - 400 K. For the studied materials, a diffuse peak in the real part $\epsilon'(T)$ of the dielectric permittivity is observed at $T_{\text{max}} \approx 315$ K. A detailed analysis of the data of $[\text{Co}(\text{C}_3\text{H}_3\text{N}_2)_2]_n$ revealed that the temperature dependence of $\epsilon'(T)$ deviates from Curie-Weiss law below ($T_{\text{max}} + 15$ K), showing a $(T - T_{\text{max}})^{-2}$ dependence. A clear dielectric dispersion occurs above $T_f \approx 287$ K and it is characterized by a distribution of relaxation times according to the Kohlrausch-Williams-Watts formula. The temperature and frequency dependence of the loss tangent $(\tan\delta)_{\text{max}}$ can be described by the Vogel-Fulcher law, indicating thermal slowing down of non-Debye dynamics. We attribute the observed dielectric properties to a relaxor ferroelectric behaviour, which is caused by the development of a freezing state below T_f . We have analysed the electrical conductivity using the Jonscher formula $\sigma(\omega) = \sigma_{\text{dc}} + A\omega^b$. The obtained results may be explained with the model, where the dc-conductivity is governed by thermally activated electrons and ac-conductivity due to the tunnelling of the overlapping large polarons. A large value of the dielectric permittivity ϵ' is found for samples absorbing the moisture from the air and the phenomenon has been associated to a cooperation between the H^+ and HCO_3^- ions and the others in the relaxation process. Due to a moisture absorption property of $[\text{Co}(\text{C}_3\text{H}_3\text{N}_2)_2]_n$, we suggest that this material is a potential candidate for a low cost room-temperature humidity sensor.

Keywords: (dielectric permittivity, electrical conductivity, cobalt complex with imidazole)

Introduction

The study of dielectric properties, including dielectric permittivities (ϵ' and ϵ'') and their relative quantities such as loss tangent $\tan\delta$ and dc- (σ_{dc}) and ac- (σ_{ac}) conductivities over a wide range of frequencies and temperatures is obviously desired for understanding the structure and dynamics of materials [1]. Specially, such an investigation on materials with an ionic conductivity character or dielectric relaxation properties is even more motivated not only by fundamental but also by applied aspects [2-5].

Some years ago, we focused our interest on magnetic properties of cobalt complexes with imidazole $\text{Co}(\text{CO}_3)(\text{H}_2\text{O})_2(\text{C}_3\text{H}_4\text{N}_2)_2$ [6] and $[\text{Co}(\text{C}_3\text{H}_3\text{N}_2)_2]_n$ [7]. The experimental data revealed that the Co^{2+} ions in these compounds behave in different manner. In the first complex, due to an unquenched spin-orbit coupling the Co^{2+} ions exhibit a large effective magnetic moment of 5.15 μ_B . The complex is characterized also by a Schottky anomaly with low-energy excitation ($\Delta/k_B = 1.3$ K), which is visible in the temperature dependence of specific heat. In contrast, the Co^{2+} ions in the latter complex are believed to be responsible for spin-glass behaviour with a spin-freezing temperature $T_{\text{sf}} = 4$ K and short-range low-dimensional antiferromagnetic behaviour characterized by a maximum at $T_{\text{max}} = 8$ K in the magnetic susceptibility. The Schottky anomaly occurs too in the compound but crystal electric field splitting is of much higher energy $\Delta/k_B \sim 200$ K.

In this work, we present results of dielectric permittivity measurements on $\text{Co}(\text{CO}_3)(\text{H}_2\text{O})_2(\text{C}_3\text{H}_4\text{N}_2)_2$ and $[\text{Co}(\text{C}_3\text{H}_3\text{N}_2)_2]_n$. It appears that the phenomena observed in these materials are quite interesting, including a relaxor ferroelectric behaviour and enhancement in the permittivity. After analysing electrical conductivity for $[\text{Co}(\text{C}_3\text{H}_3\text{N}_2)_2]_n$, we found that the charge transport takes place in the material probably by the tunnelling of the overlapping large polarons and dc-conductivity which is governed by the activation mechanism of the charge carries. Another important finding in this work is a huge effect of moisture from the air on the dielectric permittivity of $[\text{Co}(\text{C}_3\text{H}_3\text{N}_2)_2]_n$, which suggests that the studied material is a potential candidate for a low cost room-temperature humidity sensor.

Experimental details and IR spectra

- [a] Beata Świątek-Tran,
Institute of Building Engineering, Wrocław University of Technology
Wybrzeże Wyspiańskiego 27, 50-370 Wrocław, Poland
E-mail: beata.swiatek-tran@pwr.edu.pl
- [b] Hubert A. Kołodziej[†], and Andrzej Vogt
Faculty of Chemistry, University of Wrocław,
50 - 383 Wrocław, Poland
[†]deceased
E-mail: A.Vogt@chem.uni.wroc.pl
- [c] Vinh Hung Tran
Institute of Low Temperature and Structure Research
Polish Academy of Sciences, 50-950 Wrocław, Poland
Email: V.H.Tran@int.pan.wroc.pl

Samples of the $\text{Co}(\text{C}_3\text{H}_4\text{N}_2)_2(\text{CO}_3)(\text{H}_2\text{O})_2$ and $[\text{Co}(\text{C}_3\text{H}_3\text{N}_2)_2]_n$ complexes were chemically prepared from a mixture of imidazole, NaHCO_3 , H_2O and $\text{Co}(\text{NO}_3)_2 \cdot 7\text{H}_2\text{O}$. Sample preparation procedures and their characterization were described in detail before [6, 7]. These samples, henceforth abbreviated as $\text{Co}(\text{CO}_3)(\text{OH}_2)_2(\text{ImH})_2$ and $\text{Co}(\text{Im})_2$, respectively. In this work, we present the results of measurements on two samples of $\text{Co}(\text{Im})_2$ labelled as Nr 1 and Nr 2 and compare the data with that of $\text{Co}(\text{CO}_3)(\text{H}_2\text{O})_2(\text{ImH})_2$. The Nr 1 sample is an as-cast sample, but kept in air for few days and Nr 2 sample was additionally annealed in a pure nitrogen atmosphere at 150°C for 1 h just before performing impedance measurements.

The infrared spectra of studied $\text{Co}(\text{CO}_3)(\text{H}_2\text{O})_2(\text{ImH})_2$ and $[\text{Co}(\text{Im})_2]_n$ (Nr 2) samples for the wave range $50 - 4000 \text{ cm}^{-1}$ were recorded on pastille with KBr, using a Bruker IFS 66/S spectrophotometer. The observed spectra (Fig. 1) are similar to those previously reported [8, 9]. The bands found in the region 3440 cm^{-1} and $1600 - 600 \text{ cm}^{-1}$ are attributed to the vibrations of the imidazole rings. The intensive band around $3000\text{-}3200 \text{ cm}^{-1}$ due to the bridging mode $\text{H}_2\text{O}-\text{CO}_3$ is observed in IR spectrum of $\text{Co}(\text{CO}_3)(\text{H}_2\text{O})_2(\text{ImH})_2$ only. The evidence for the complex feature is the presence of the strong peak at wavenumbers $\sim 250 \text{ cm}^{-1}$ in $\text{Co}(\text{CO}_3)(\text{H}_2\text{O})_2(\text{ImH})_2$ and $\sim 350 \text{ cm}^{-1}$ in $[\text{Co}(\text{Im})_2]_n$. This band corresponds to the stretching frequency $\nu(\text{Co}-\text{N})$. Comparing to the vibrating data of the free imidazole one recognizes that some wavenumbers of the studied complexes are shifted, confirming the presence of Co-N coupling mode.

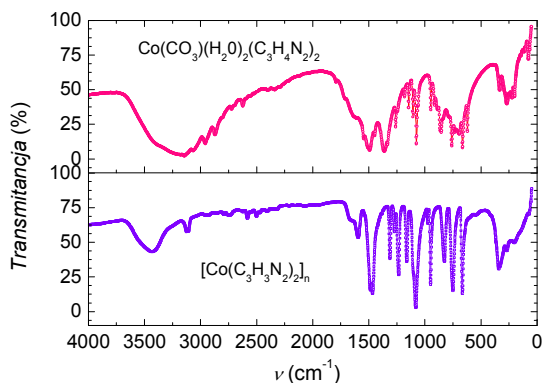


Fig. 1 IR spectra of $\text{Co}(\text{CO}_3)(\text{H}_2\text{O})_2(\text{ImH})_2$ and $[\text{Co}(\text{Im})_2]_n$.

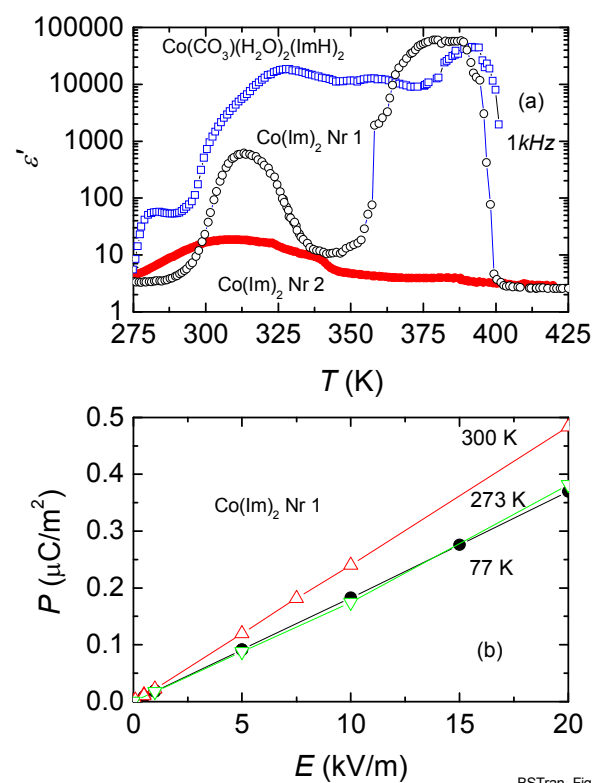
Electric permittivity was obtained from impedance measurements in the frequencies up to 1000 kHz and oscillation voltage up to 20 V, using an autobalance bridge HP 4284A LCR meter. For the measurements the samples of a typical diameter of 8 mm and thickness of $\sim 1 \text{ mm}$ were coated with silver paint or copper foil electrodes. The samples were placed between two pure copper sheets and were connected to the bridge by four coaxial cables. The complex permittivity and conductivity were calculated after proper calibration using standard Teflon sample. The error in the absolute value of complex permittivity was less than 5%. All of the measurements were performed on a heating run from 80 to 400 K using a rate of 0.5 deg/min . The thermocouple Cu-

constantan, calibrated with a calibrated cernox resistor, was kept near the sample, and was used to control the temperature within the experimental error of 0.2 deg .

Results and discussions

Frequency- and temperature dependent dielectric permittivity

In Fig. 2(a) we present the temperature dependence of the real part $\epsilon'(T)$ of the dielectric permittivity of two samples of $\text{Co}(\text{Im})_2$ measured at a frequency of $\omega = 1 \text{ kHz}$. In this figure we also compare the permittivity data with that of $\text{Co}(\text{CO}_3)(\text{H}_2\text{O})_2(\text{ImH})_2$. As can be seen from this figure, ϵ' of Nr 1 sample exhibits two anomalies; one is located between 360 K and 390 K and the other is centred at $T_{\text{max}} \sim 315 \text{ K}$.



BSTran_Fig_2

Fig. 2 a) Temperature dependence of the real part of the dielectric permittivity of $\text{Co}(\text{CO}_3)(\text{H}_2\text{O})_2(\text{ImH})_2$ and $\text{Co}(\text{Im})_2$ at a frequency 1 kHz. b) The isothermal polarization as a function electric fields for $\text{Co}(\text{Im})_2$ (sample 1). The solid lines are guides for eyes.

The remarkable feature of the first anomaly is its giant relative value, reaching a value of $\sim 10^4$, i.e., of the same order of magnitude as those of any high-permittivity classical dielectric materials ($\text{KNaC}_4\text{H}_4\text{O}_6 \cdot 4\text{H}_2\text{O}$, KH_2PO_4 , SrTiO_3 and BaTiO_3) or of other relaxor ferroelectrics $\text{KTa}_{1-x}\text{Nb}_x\text{O}_3$, [10] and $\text{PbMg}_{1/3}\text{Nb}_{2/3}\text{O}_3$ [11]. The observed ϵ' -value in Nr 1 sample is also comparable to those of the quasi-1D organic molecules tetramethyltetrathiafulvalence $(\text{TMTTF})_2\text{X}$ with $\text{X} = \text{Br}$, [12] and PF_6 [13]. For the latter compounds, a large ϵ' -values have been interpreted as either a result of short-range charge

density wave (CDW) states or a formation of a charge ordered state of Wigner crystal type due to long-range Coulomb interaction. In our case, the origin of the large ϵ' -value at the high-temperature (HT) anomaly might be another. Usually, a large value of ϵ' could be related to the ionic nature and/or an artifact due to electrode surface effects. With both silver paints and rigid Cu electrodes, the investigated $\text{Co}(\text{CO}_3)(\text{OH}_2)_2(\text{ImH})_2$ and $\text{Co}(\text{Im})_2$ (Nr 1) samples have similar responses. It provides that the measured properties of the materials are intrinsic. Further, as can be inferred from the magnetic susceptibility measurements of the $\text{Co}(\text{Im})_2$ (Nr 1) sample [14] (not shown here) and from a comparison to the permittivity data of the Nr 2 sample and as well as of $\text{Co}(\text{CO}_3)(\text{OH}_2)_2(\text{ImH})_2$, the HT-anomaly in Nr 1 sample is presumably related to H_2O and CO_2 contaminations from moist air. On the other hand, we remember that both H_2O and CO_2 themselves cannot give so high dielectric permittivity values [15]. This means that the motion of charges Co^\oplus and Im^\ominus must be mainly responsible for the observed phenomenon. One of possibilities to explain the role of H_2O and CO_2 is that the charges resulting from the reaction $\text{H}_2\text{O} + \text{CO}_2 \rightarrow \text{H}^+ + \text{HCO}_3^-$ may cooperate with other charges, giving a rise to the large ϵ' -values. This interpretation might be supported considering the temperature dependence of ϵ' of $\text{Co}(\text{CO}_3)(\text{OH}_2)_2(\text{ImH})_2$. For which, ϵ' exhibits as many as three anomalies, at around 275 K, 325 K and at 390 K, where the sample starts to decompose. The presence of the anomaly at 275 K for $\text{Co}(\text{CO}_3)(\text{OH}_2)_2(\text{ImH})_2$ can be ascribed to H_2O in this compound.

As far as we consider the dielectric behaviour of $[\text{Co}(\text{Im})_2]_n$, we see that the anomaly at T_{max} is characterized by a broad maximum. It is worth to underline that the values of ϵ' at this maximum may vary by a factor of 5 between samples, depending on the degree of air absorption. We found that ϵ' of very freshly prepared Nr 2 sample remains at low as a value of about 18 shown in Fig. 2 (a). We emphasize the fact that the polarization of each sample at 300 K is linear in electric fields, at least, up to 20 kV/m as indicated in Fig. 2(b), so that the difference in the ϵ' -values is certainly due to an amount of the absorbed H_2O and CO_2 from the moist air. This observation suggests that $[\text{Co}(\text{Im})_2]_n$ could be a promising candidate for a room-temperature humidity sensor. In Fig. 2(b), we show also the isothermal polarization measured at 77 K and at 273 K. A comparison of those two curves reveals that they are similar in the magnitude, i.e., the dielectric permittivity practically does not depend on the temperature in the temperature range 77 - 273 K.

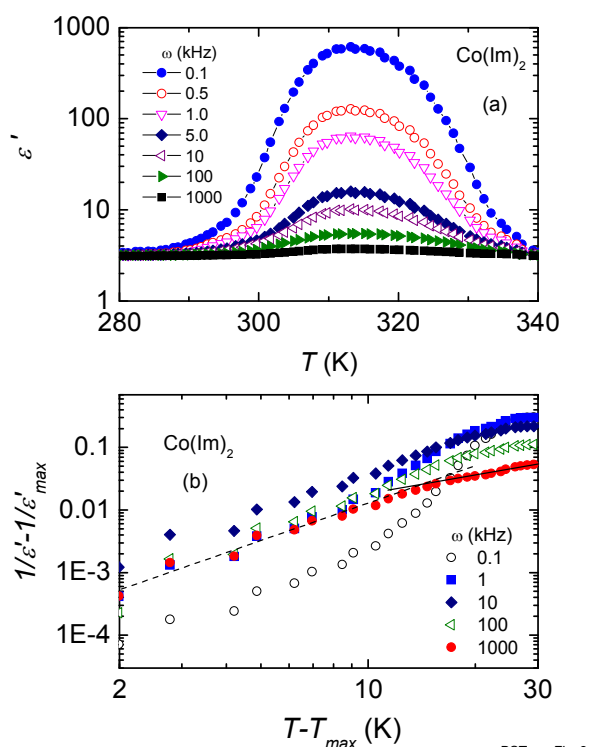
In Fig. 3(a) we show the permittivity of the Nr 1 sample as a function of frequency between 0.1 and 1000 kHz. We found that below 280 K there is no any signal of the dielectric relaxation for the studied frequency range. However, a dielectric dispersion appears just above ~ 285 K and exhibits a maximum at $T_{\text{max}} \sim 315$ K. It is clear that the intensity of T_{max} depends on frequency. Because the Debye theory has assumed a constant number of oscillators with a single relaxation time, the observed phenomenon clearly rules out the dielectric relaxation of a Debye type. In fact the $\epsilon'(\omega, T)$ and $\tan\delta(\omega, T)$ -dependencies (see Fig. 5) resemble those of various other relaxor ferroelectrics, in which the divergence of ϵ' and

$\tan\delta$ occurs when the system approaches to a characteristic temperature T_{max} [10, 11].

Relaxor ferroelectrics are known also to show non Curie-Weiss behaviour of the dielectric susceptibility above T_{max} [16-20]. In so-called compotional heterogeneity model, Smolensky [16] predicted a $1/\epsilon \propto (T-\Theta)^\gamma$ relationship, where γ was approximately two and Θ is the paraelectric temperature Curie. The deviation from Curie-Weiss behaviour may be also investigated using the approach given by Randall et al. [20]:

$$\frac{1}{\epsilon'} - \frac{1}{\epsilon'_{\text{max}}} = \frac{(T-T_{\text{max}})^2}{2\eta\omega_{\text{max}}} \quad (1)$$

where η is the diffuseness parameter characterizing the diffuse phase transition. In Fig. 3(b) we show the $(1/\epsilon' - 1/\epsilon'_{\text{max}})$ vs $(T - T_{\text{max}})$ in the log-log scale. The plots reveal two temperature regions: above $\sim (T_{\text{max}}+15$ K) ϵ' obeys the Curie-Weiss law, whereas in the temperature range $T_{\text{max}} - (T_{\text{max}}+15$ K), $1/\epsilon'$ follows the $(T - T_{\text{max}})^2$ -dependence. The latter feature undoubtedly is an indication that electric correlations between dipoles occur relatively far above T_{max} . We notice that the $(T - T_{\text{max}})^2$ dependence is valid for the entire investigated frequency range, but the value of the parameter η increases with increasing frequency, reaching to about 40 K at $\omega = 1000$ kHz.



BSTran_Fig_3

Fig. 3 (a) Temperature dependence of the real part of the dielectric permittivity of $\text{Co}(\text{Im})_2$ (sample 1) at different frequencies. (b) Log-log plots of $(1/\epsilon' - 1/\epsilon'_{\text{max}})$ vs $(T - T_{\text{max}})$ for $\text{Co}(\text{Im})_2$ at various frequencies. The dashed and solid lines have slopes of -2 and -1, respectively.

In Fig. 4 we show the standard Cole-Cole plots where ϵ'' is a function of ϵ' for several temperatures. This figure illustrates the evolution of the dielectric relaxation with increasing

temperature. It is obvious that the shape ϵ'' vs ϵ' curves indicates an asymmetry of the relaxation spectrum. A widely established explanation for this kind of the behaviour is that there is a distribution of relaxation times. To support the validity of this statement for $\text{Co}(\text{Im})_2$ we have tested the formula of Kohlrausch-Williams-Watts [21, 22]:

$$\epsilon^*(\omega) = \epsilon_\infty + (\epsilon_0 - \epsilon_\infty) \int_0^\infty \exp(-x) \exp[-i(\omega\tau_0)x^{1/\beta}] dx \quad (2)$$

to our experimental data. In Eq. (2), $\epsilon^*(\omega)$ is the complex dielectric permittivity at frequency ω , while ϵ_0 and ϵ_∞ are the dielectric permittivities at frequencies much lower and higher than the mean frequency of the relaxation $\omega_0 = 1/\tau_0$, and the β denotes the Kohlrausch exponent parameter. We calculated $\epsilon^*(\omega) = \epsilon'(\omega) - i\epsilon''(\omega)$ from the experimental ϵ' and ϵ'' values. In our case, owing to a significant contribution of the dc-conductivity to ϵ'' , we firstly extracted the dielectric relaxation $\epsilon''(\omega)$ from the raw data by the relation $\epsilon''(\omega) = \epsilon''(\omega)_{\text{raw}} - \sigma_{\text{dc}}/\epsilon_0\omega$, where ϵ_0 is the dielectric constant of the free space. The results of simulation of the Eq. (2) are shown in Fig. 4 as solid lines.

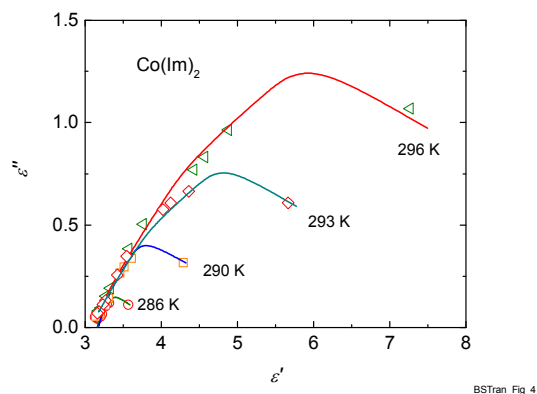


Fig. 4 Complex-plane plots of the real ϵ' and imaginary ϵ'' parts of dielectric permittivity at several temperatures. The solid lines present fits of the data to the Kohlrausch-Williams-Watts formula.

The agreements between the theoretical and the experimental values were satisfactory. The β -value equals to ~ 0.58 and seems to be independent of the temperature. It is worthwhile to add that the exponent $\beta \equiv 1 - n$ correlates with the coupling parameter n , which in terms of the coupling model [23], describes the degree of correlations between ions. For a number of ionic glasses, the correlation between the thermally activated energy and the exponent β has also been reported [24].

The temperature dependence of $\tan\delta = \frac{\epsilon''}{\epsilon'}$ of the Nr 1 sample at different frequencies is shown in Fig. 5(a). In a similar manner to $\epsilon'(\omega, T)$ -dependences, the intensity of $(\tan\delta)_{\text{max}}$ strongly decreases with increasing frequency. A remarkable feature of this figure is the occurrence of two maxima; for $\omega = 100$ Hz the first maximum appears at $T_{m1} \sim 301$ K and the second at $T_{m2} \sim 330$ K. As the frequency is increased T_{m1} increases up to ~ 315 K at $\omega = 1000$ kHz. For the Nr 2 sample, the temperature dependence of $\tan\delta$ closely resembles that of the Nr 1 sample. For the Nr 2 sample, we observe also two characteristic loss peaks but with a narrower

temperature window of 310 - 325 K. With increasing frequency these loss peaks become superimposed on one broader maximum. It appears that the position of $T_{\text{max}2} = 325$ K seems to be less sensitive on increasing frequency. The difference between two samples also arises in the absolute value of the loss tangent, i.e., $\tan\delta$ of the Nr 2 sample reaches approximately 4, a value that is by a factor of 4 smaller than observed for the Nr 1 sample.

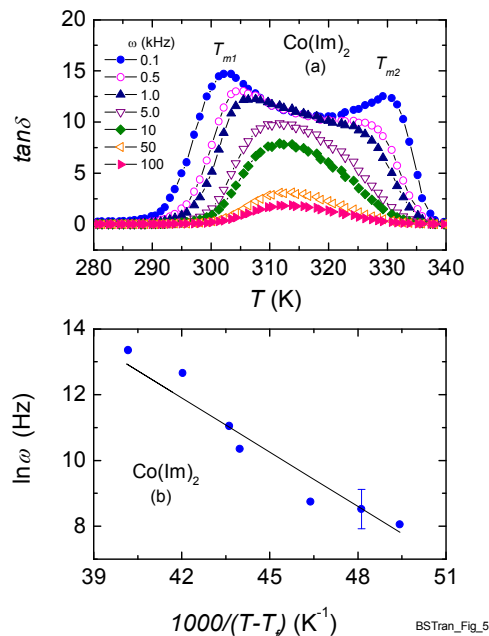


Fig. 5 (a) Temperature dependence of the $\tan\delta$ of $\text{Co}(\text{Im})_2$ at various frequencies. (b) Temperature dependence of the mean relaxation time in $\text{Co}(\text{Im})_2$. The solid line corresponds to the activated Vogel-Fulcher law with an energy 550 K and a freezing temperature 285 K.

For description of the dielectric relaxation of T_{m1} we have used the phenomenological Vogel-Fulcher law [25]:

$$\omega(T_m) = \omega_0 \exp[-E_a/k_B(T_m - T_f)] \quad (3)$$

where ω is a frequency at which $\tan\delta$ reaches its maximum value. As usual, this frequency corresponds to some mean value of the relaxation time of charge polarization. The remaining parameters ω_0 , E_a , k_B , T_m and T_f denote an attempt frequency, an activation energy, Boltzmann constant, the position of $\tan\delta$ maximum and a freezing temperature, respectively. In Fig. 5(b) we show the results of fitting of T_{m1} with Eq. 3 for the Nr 1 sample. The fitting parameters are $\omega_0 = 2.37 \times 10^{15}$ Hz, $E_a = 550$ K (44 meV) and $T_f = 285$ K. We note that similar orders of the magnitude of E_a and ω_0 were found in the Nr 2 sample. The fulfilment of experimental data to the Eq. 3 indicates the slowing down of the relaxation process on approaching the freezing temperature T_f . However, it is particularly interesting that the determined experimentally parameters imply to ascribe the observed loss anomalies to polaroniclike relaxations. There are two premises: First, the obtained activation energy is small, and this directly precludes an eventual relaxation process due to ion jumping.

For the latter process, at least the binding energy, which requires to leave the bond must be of the order of 0.5 - 1 eV. Second, the value of the attempt frequency ω_0 markedly exceed the characteristic phononic frequencies (10^{12} Hz). This means that the relaxation should be connected to the charge carries, likely polarons which may move by hopping tunnelling. It is noteworthy that in some perovskites, where a polaronic mechanism has been considered [26, 27], the magnitude of E_a and ω_0 were found to be the comparable order to our finding.

dc- and ac conductivity

Fig. 6 shows the temperature dependence of the real part $\sigma'(\omega)$ of the electrical conductivity, which is calculated from the imaginary part $\varepsilon''(\omega)_{raw}$ of the dielectric permittivity via relation:

$$\sigma'(\omega) = \varepsilon_0 \omega \varepsilon''(\omega)_{raw} \quad (4)$$

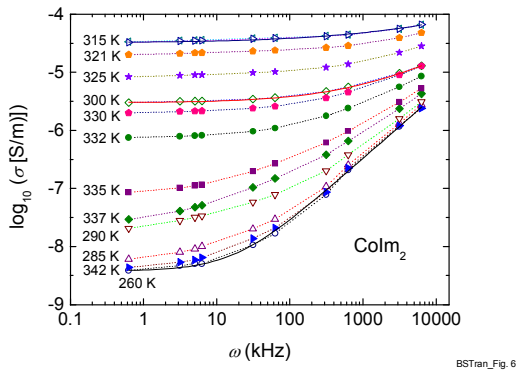


Fig. 6 Frequency dependence of the real part of the conductivity at different temperatures for the Nr 1 $\text{Co}(\text{Im})_2$ sample. The solid lines are representative fits using eq. 5 as described in the text.

Qualitatively, the frequency dependence of $\sigma'(\omega)$ at different temperature is similar to each other. At low frequencies σ' is practically independent of ω , indicating that the conductivity includes a considerable contribution of dc conductivity. But in the high-frequency region the $\ln\sigma'$ vs. $\ln\omega$ plots are linear, which clearly indicate the dominated contribution of the ac-conductivity. Thus, we may analyse the conductivity in the framework of the Jonscher's universal formula [28, 29]:

$$\sigma'(\omega) = \sigma_{dc} + \sigma_{ac}(\omega) = \sigma_{dc} + A\omega^s \quad (5)$$

where A is a temperature dependent parameter and s is a frequency exponent with values taking between 0 and 1. We have fitted the Eq. (5) to the experimental data. The solid lines in Fig. 6 represent the theoretical curves for a few representative temperatures. Further analyse of the fitted parameters σ_{dc} and s will be given below.

The values of σ_{dc} are shown in Fig. 7, as $\ln(T\sigma_{dc})$ vs. $1/T$. We note that the dc-conductivity is strongly temperature dependent. For instance, the Nr 1 sample shows its maximum value of the conductivity of $\sim 4 \times 10^{-5}$ S/m at 313 K, but at low temperatures a depression of σ_{dc} drops down to below 10^{-9}

S/m. A similar temperature behaviour of the dc-conductivity is observed for the Nr 2 sample. In this case, the low-temperature and room temperature conductivity amounts roughly to 10^{-9} and 9×10^{-6} S/m, respectively. This big change of σ with temperature assigns a thermally excitation of charge carriers from the lower energy valence band to the higher energy conduction band. Indeed, when we inspect the figure 7 we found a linear dependence between $\ln(T\sigma_{dc})$ and $1/T$ for both the samples. In according to the gap function of the dc-conductivity:

$$\sigma'(\omega) = \frac{\sigma_0}{T} \exp(-E_a/k_B T) \quad (6)$$

we obtain activation energies E_a of 3.1 and 2.2 eV for the Nr 1 and Nr 2 samples, respectively. These values are obvious larger than the value of the activation energy derived from the relaxation process as considered above, and would give an evidence of semiconducting gap.

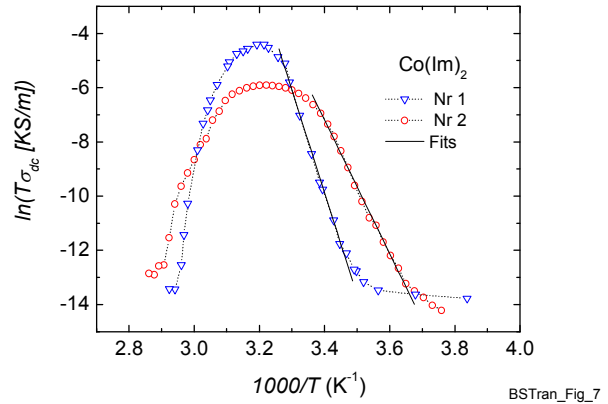


Figure 7: Temperature dependence of the dc conductivity as a function $\ln(T\sigma_{dc})$ vs T^{-1} for $\text{Co}(\text{Im})_2$. The solid lines are fits to eq. (6) described in the text.

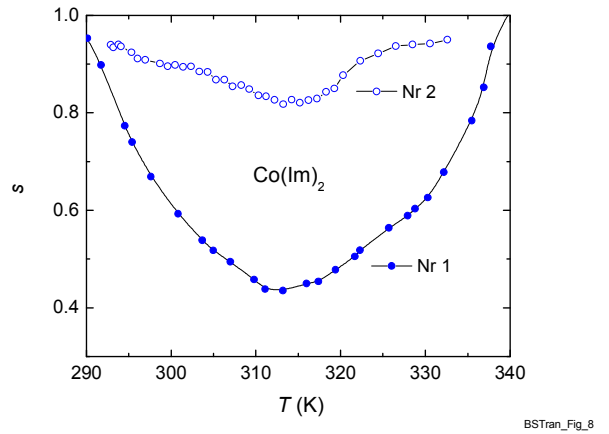


Figure 8: Temperature dependence of the frequency exponent s of two samples of $\text{Co}(\text{Im})_2$.

The physical interests can be seen from the figure 8, where we present the fitted s -values as function of temperature for the both Co(Im)₂ measured samples. The major point on $s(T)$ -curves is distinct minimum around T_{max} . There are several theoretical models [30, 31], which anticipate a strong temperature dependence of s , but only one called the overlapping large polaron tunnelling (OLPT) model which predicts a minimum in the $s(T)$ -dependence. In this model, the large-polaron wells at two sites are assumed to overlap, thus they reduce the polaron hopping energy, which is given by $W_H = W_{HO}(1 - r_0/R)$, where, W_{HO} is a constant, r_0 is the radius of a large polaron and R is the intersite separation. The ac conductivity and the frequency exponent s in this model read [30, 31]:

$$\sigma'_{ac} \propto \frac{(\pi^2 ek_B T)^2}{12} \frac{\omega R_h^4}{2\alpha k_B T + W_{HO} r_0 / R_h^2} \quad (7)$$

and

$$s = 1 - \frac{8\alpha R_h + 6W_{HO} r_0 / R_h k_B T}{(2\alpha R_h + W_{HO} r_0 / R_h k_B T)^2} \quad (8)$$

where α is the decay parameter of the electron wave function and R_h is the hopping length at the frequency ω . From Eq. 8 one sees that s reaches unity as $T \rightarrow 0$ K, and shows up a minimum at a certain temperature for a small values of r_0 . Thus, the temperature dependence of $s(T)$ of Co(Im)₂ seems to be reasonably interpreted in terms of OLPT model.

Concluding remarks

The main results of the dielectric and conductivity investigation on Co(Im)₂ can be summarized as follows:

- i) A diffuse maximum in the real part of the permittivity occurs at $T_{max} \sim 315$ K, and its intensity depends on the degree of the moisture absorption and on applied frequencies.
- ii) Two dielectric anomalies are observed in the temperature dependence of $\tan\delta$. An analysis of the data with the Vogel-Fucher formula indicates a slowing down of the relaxation process.
- iii) The dielectric relaxation starts to show up from the freezing temperature $T_f \sim 287$ K. Its asymmetric spectrum reflects the energy distribution of relaxation times.
- iv) The dc conductivity shows a simple activated temperature dependence. The observed activation energy of $\sim 2 - 3$ eV implies the presence of the semiconducting gap.
- v) The ac conductivity obeys an equation $\sigma_{ac}'(\omega) = A\omega^s$.

The observation (i) strongly suggest that Co(Im)₂ may be a good candidate for the room-temperature capacitive sensor for measurements of the moisture. The results listed in (i – iii) are typical of relaxor ferroelectrics. However, analysing different relaxor ferroelectrics from the point of view of the

dielectric behaviour, it appears that none of the well-known mechanisms attributing to the dielectric response is unambiguous, and therefore the determination of the proper mechanism for a given system is not easy task. For instance, the relaxor PbMg_{1/3}Nb_{2/3}O₃ is just one of the classical relaxors that was considered at the beginning in terms of (1) superparaelectric model [32]. In the other word, the material is composed of ferroelectric clusters being embedded in a paraelectric matrix. However, measurements on single crystals [33] have indicated that the vibration of the boundaries of the polar regions is the governing mechanism, thus, it favours (2) the interphase boundary motion model [34, 35]. There exist other possible models, which have been proposed for relaxors so far: (3) dipole glass [36, 37], and (4) dipolar dielectric with random fields [38, 39]. We might point out that model (3) appears to be a good description for KTa_{1-x}Nb_xO₃ [10] and model (4) probably takes its role in Rb_{1-x}(ND₄)_xD₂PO₄ [40]. Examining Co(Im)₂ we see that in addition to the evidence of the freezing feature as summarized in (i)-(iii), other characteristic property of a dipole glass is a dielectric susceptibility that begins to deviate from CW law at temperatures much larger than T_f . This feature happens in Co(Im)₂ at temperatures as high as about 40 K above T_f . Therefore, it is legitimate to propose the interpretation of the dielectric data on Co(Im)₂ in terms of the dipole glass model. However, we have to admit that alternative explanation of the experimental data could be taken into account, e.g., in terms of the random-bond random-field model. The fact that in the complex Co(Im)₂ is an amorphous low-dimensional material [7], may be a reason for different local random fields, which would lead to a frustration of dipolar interactions, and in consequence result in the relaxor state.

Let us consider now the dc and ac conductivity behaviour of Co(Im)₂. As we summarized in (iv) the dc conductivity has given evidence for a semiconducting gap. In an attempt to understand this behaviour, it seems useful to recall the spectroscopic data reported by Baraniak et al. [41]. Accordingly, the electronic UV spectrum of Co(Im)₂ displays a broad band in the ultraviolet region, pointing to an interband transition and this feature may hint at strong p_π - d_π - p_π interactions between the imidazole ligands *via* the bridging Co²⁺ ions. In a classical argumentation, the d -symmetry orbitals willingly overlap with the $2p$ -orbitals of the imidazole. The valence band could be formed with the hybridized set of the $4s$ -orbitals of Co and $2p$ -orbitals of the imidazole, whereas the conduction band comprising of the anti-bonding sp -band is empty. The position of the Fermi level is situated just above the non-bond d -band of the Co ions. This model might help us in an image of the gap state found in the dc conductivity. We found an exponential increase of the ac conductivity with frequency. This behaviour has been described to relaxations caused by the motion of electrons or atoms, associated with hopping or tunnelling [30, 31]. The finding of the minimum in $s(T)$ around 315 K suggests that the OLPT model might be invoked to explain the ac conductivity phenomenon in Co(Im)₂.

Finally, it would be interesting to compare the dielectric and magnetic data between Co(CO₃)(OH₂)₂(imH)₂ and

Co(Im)₂, and as well as between Co(Im)₂ and Cu(Im)₂ and Zn(Im)₂. The Co-based compounds are both paramagnetic at room temperature, but possessing different values of the effective magnetic moment μ_{eff} . An unquenched spin-orbit coupling was assumed to be the reason of a larger μ_{eff} in Co(CO₃)(OH₂)₂(imH)₂ [6]. Considering the fact that the latter complex has also a larger permittivity ϵ' at room temperature may suggest that the dielectric properties are associated with the Co²⁺ orbitals, which in fact are involved in the dipole of Co – ligands. When we deal with the Cu(Im)₂ and Zn(Im)₂ complexes, we see that the paramagnetic properties of Cu²⁺ [42] correlate with lower ϵ' -value of 2.5 – 3.2 in Cu(Im)₂ [43] compared to that of Co(Im)₂, while the diamagnetic properties due to zero magnetic moment of Zn²⁺, correspond to extremely low ϵ' -value of only 2.3 in Zn(Im)₂ [44]. So, the weaker magnetic interactions between magnetic ions, the smaller dielectric permittivity there is in these complexes, and this observation put forward the magnetic role of central metal ions on the dielectric properties across the Co²⁺, Cu²⁺, and Zn²⁺ complex series. Furthermore, the effect of different ligands seems to be also intriguing and further investigations of complexes, for instance, with pyrazole as the ligand are strongly desired.

Notes and references

1. C. J. F. Böttcher and P. Bordewijk: *Theory of Electric Polarization*, Vol. I & II. Verlag Elsevier, Amsterdam, Oxford, New York, 1978.
2. Z. Gadjourova, Y. G. Andreev, D. P. Tunstall and P. G. Bruce, *Nature* 2001, **412**, 520-523.
3. N. Zheng, X. Bu and P. Feng, *Nature* 2003, **426**, 428-432.
4. M. Li, M. J. Pietrowski, R. A. De Souza, H. Zhang, I. M. Reaney, S. N. Cook, J. A. Kilner and D. C. Sinclair, *Nature Mater.*, 2014, **13**, 31-35.
5. J Wang, Yu-Shi He, and J. Yang, *Adv. Mater.*, 2014, 1 – 7.
6. B. Świątek-Tran, H. A. Kołodziej, V. H. Tran, M. Baenitz, A. Vogt, *phys. status solidi a* 2003, **196**, 232-235.
7. V. H. Tran and B. Świątek-Tran, *Dalton Trans.*, 2008, **36**, 4860 - 4865.
8. A.M. Vecchio-Sadus, *Trans. Met. Chem.*, 1995, **20**, 46 – 55.
9. M. Cordes, J.L. Walter, *Spectrochim. Acta A*, 1968, **24**, 237 - 252.
10. J. Toulouse, X.M. Wang, L.A. Knauss, and L.A. Boatman, *Phys. Rev. B* 1991, **43**, 8297 – 8302.
11. R. Sommer, N.K. Yushin, and J.J. van der Klink, *Phys. Rev. B* 1993, **48**, 13230 – 13237.
12. F. Nad', P. Monceau, and J.M. Fabre, *Eur. Phys. J. B* 1998, **3**, 301 - 306.
13. F. Nad', P. Monceau, C. Carcel, and J.M. Fabre, *Phys. Rev. B* 2000, **62**, 1753 – 1756.
14. Due to a relieving of H₂O, magnetic susceptibility shows a discontinuous drop at around 375 K – information to be provided on request.
15. D.R. Lide and H.P.R. Frederikse, red. *Handbook of Chemistry and Physics*, CRC Press, New-York, 1977, pp. 6-188.
16. G. Smolensky, *J. Phys. Soc. Jpn. Suppl.* 1970, **28**, 26 – 37.
17. G. Jonker, *Mater. Res. Bull.* 1983, **18**, 301 – 308.
18. B. Kirsh, H. Schmitt, and H. Muser, *Ferroelectrics* 1986, **68**, 275 - 284.
19. D. Viehland, S. J. Jang, L. E. Cross, and M. Wuttig, *Phys. Rev. B*, 1992, **46**, 8003 - 8006.
20. C.A. Randall, A.D. Hilton, D.J. Barber, T.R. Shrout, *J. Mater. Res.* 1993, **8**, 880 – 884.
21. G. Williams and D.C. Watts, *Trans. Faraday Soc.*, 1970, **66**, 80 - 85.
22. G. Williams, D.C. Watts, S.B. Dev and A.M. North, *Trans. Faraday Soc.*, 1971, **67**, 1323 -1335.
23. K.L. Ngai, A.K. Rajagopal, and S. Teitler, *Nucl. Phys. B (Proc. Suppl.)* 1988, **5**, 103 – 108.
24. K.L. Ngai, J.N. Mundy, H. Jain, O. Kanert, and G. Balzer-Jollenbeck, *Phys. Rev. B* 1989, **39**, 6169 - 6179; K.L. Ngai and S.W. Martin, *ibid*, 1989, **40**, 10550 - 10556.
25. J. L. Tholence, *Solid State Commun.*, 1980, **35**, 113 - 118.
26. E. Iguchi, N. Kubota, T. Nakamori, N. Yamamoto, and K.J. Lee, *Phys. Rev. B*, 1991, **43**, 8646 - 8649.
27. O. Bidault, M. Maglione, M. Actis, M. Kchikech, and B. Salce, *Phys. Rev. B*, 1995, **52**, 4191 - 4197.
28. A.K. Jonscher, *Colloid Polymer Sci.*, 1975, **253**, 231 – 250.
29. A. K. Jonscher, *Nature*, 1977, **267**, 673 – 679.
30. A.R. Long, *Adv. Phys.*, 1982, **31**, 553 - 637.
31. S.R. Elliott, *Adv. Phys.*, 1987, **36**, 135 - 218.
32. L.E. Cross, *Ferroelectrics*, 1987, **76**, 241 - 267; *ibid*, 1994, **151**, 305 - 320.

- [4] 33. A.K. Tagantsev and A.E. Glazounov, *Phys. Rev. B*, 1998, **57**, 18 - 21.
- [5]
- [6] 34. V. Westphal, W. Kleemann, and M.D. Glinchuk, *Phys. Rev. Lett.*, 1992, **68**, 847 - 850.
- [7]
- [8] 35. A.E. Glazounov, A.K. Tagantsev, and A.J. Bell, *Phys. Rev. B*, 1996, **53**, 11281 - 11284.
- [9]
36. D. Viehland, S.J. Jang, L.E. Cross, and M. Wuttig, *J. Appl. Phys.*, 1990, **68**, 2916 - 2921.
37. H. Gui, B. Gu, and X. Zhang, *Phys. Rev. B*, 1995, **52**, 3135 - 3142.
38. B.E. Vugmeister and H. Rabitz, *Ferroelectrics*, 1997, **201**, 33 - 42.
39. M.D. Glinchuk, and V.A. Stephanovich, *Ferroelectrics Lett.*, 1992, **22**, 113 - 119.
40. Z. Kutnjak, R. Pirc, A. Levstik, I. Levstik, C. Filipič, R. Blinc, and R. Kind, *Phys. Rev. B*, 1994, **50**, 12421 - 12482.
41. E. Baraniak, H.C. Freeman, J.M. James, and C.E. Nockolds, *J. Chem. Soc. A*, 1970, 2558 - 2566.
42. B. Świątek-Tran, H. A. Kołodziej, V. H. Tran, *Czechoslovak J. Phys.* 54 (2004) D547-550.
43. B. Świątek-Tran, *PhD thesis*, Faculty of Chemistry, University of Wrocław, 2005.
44. B. Świątek-Tran, H.A. Kołodziej, V.H. Tran, *J. Solid State Chem.* 177 (2004) 1011 - 1016
- Received: ((will be filled in by the editorial staff))
Published online: ((will be filled in by the editorial staff))
-

